Current Applied Physics 14 (2014) 1318–1324

Contents lists available at ScienceDirect

Current Applied Physics

journal homepage: www.elsevier.com/locate/cap

Influence of thickness and crystalline structure on thermal and optical properties of ZnO thin films

K.I. Mohammed [b], F.M. Jasim [a], M.I. Azawe [a, *]

[a] Department of Physics, College of Education, Mosul University, Iraq
[b] Department of Physics, College of Science, Kirkuk University, Iraq

ARTICLE INFO

Article history:
Received 13 April 2014
Received in revised form
3 July 2014
Accepted 3 July 2014
Available online 12 July 2014

Keywords:
ZnO thin film
Optical properties
Heat equation
Photothermal deflection technique
Thermal diffusivity
Temperature gradient of refractive index

ABSTRACT

Measurements of the temperature dependence of refractive index of ZnO thin films and thermal diffusivity using photothermal deflection technique are presented. Thin film thickness and surface homogeneity were found to be the effective parameters on optical and thermal properties of the thin films. High refractive index gradient with temperature was found for films of a nonuniform distribution and gathered in clusters, and a high predicted value for thermal diffusivity. Optical properties of the thin films revealed that films with disorder in the deposition and gathered clusters showed poor transmittance in visible region with a pronounced peak in the near IR, and also a reduction in the band gap. A detailed parametric analysis using analytical solution of one-dimensional heat equation had been performed. A discontinuity in the temperature elevation at the ZnO-glass interface was found.

1. Introduction

Photothermal deflection technique (PTD) is a well-known sensitive method for obtaining both the thermal and optical parameters of a substance. It has been used recently for measuring small absorption [1], temporal response of a nonlinear refraction of materials [2], thermal effusivity of vegetable oils [3], characterizing heat conduction in biological tissue [4]. PTD is an attractive optical contactless method based on the pump-probe technique, with a pump laser for initiation of the surface thermal deformation that is chopped mechanically, and a probe laser for deflection by passing through the thermal lens [5], provided that PTD is in its Gaussian heating [6].

This technique will be implemented for the investigation of the thermal and optical characteristics of thin film ZnO. ZnO-based transparent conducting oxides (TCOs) have been the object of significant research activities for solar cells and flat panel displays, due to the low cost and abundance [7]. ZnO conducting oxide is an n-type transparent semiconductor material with a wide direct band gap of 3.37 eV and a large exciton binding energy of 60 meV at room temperature [8] making it as high level of transparency in the visible and near-IR region. Moreover, it is stable upon exposure to high energy radiation and wet chemical etching [9]. More recent applications of ZnO thin films have been found [10]. Thin films of ZnO have been grown by many deposition technique including molecular beam epitaxy, chemical vapor deposition (CVD), vacuum evaporation, and spray pyrolysis [11].

A characteristics one-dimensional heat equation in the different media when illuminated perpendicularly by modulated pump laser for studying the energy density absorbed by undoped-ZnO will be used [12]. Thermal properties of ZnO thin films are important novel physical properties as well as its technological implications in many fields. Thermal induced effects on the surface and transient heat diffusion of the thin film can be monitored directly by PTD [13–15].

This article presents an easy way to estimate the optical and thermal of ZnO thin film and to provide a comparison between films of different grain size, film thickness, and crystalline structure. Film thickness effects will be investigated in terms their thermal diffusivity and refractive index change with temperature. The article starts by presenting a characteristic equation based on one-dimensional heat equation for the sample/substrate interface. Analytical solution will be to obtain temperature elevation at the ZnO-glass interface.

* Corresponding author.
E-mail addresses: fathephy@yahoo.com, muzahim_935@yahoo.com (M.I. Azawe).

http://dx.doi.org/10.1016/j.cap.2014.07.007
1567-1739/

2. Theory

One-dimensional heat flow will be considered when the pump laser energy was absorbed on the irradiated thin film surface, resulting a temperature gradient detected by the deflection of the probe beam. Thin film samples of ZnO material were deposited on thick glass substrate by CVD. The analysis will be based on assuming the continuity of the temperature and heat flow through the fluid (air)-ZnO-glass at the different interfaces, as shown in Fig. 1.

The characteristics one-dimensional heat equation in different media when illuminated perpendicularly by modulated pump laser can be written as [Eq. (5) of Ref. [12] with $\tau_T = 0$] taking into account the relaxation of heat flux:

$$\frac{\tau_q}{D_i}\frac{\partial^2 T}{\partial t^2}+\frac{1}{D_i}\frac{\partial T}{\partial t}=\frac{\partial^2 T}{\partial z^2}+\frac{1}{k_i}\left(S+\tau_q\frac{\partial S}{\partial t}\right), \tag{1}$$

where D_i is the thermal diffusivity. The subscript $i = a$ (air, the surrounding medium), g (substrate glass), and s (sample). Thermal diffusivity in terms of the thermal conductivity k_i:

$$D_i=\frac{k_i}{\rho_i C_{pi}}. \tag{2}$$

ρ is the density, and C_p is the heat capacity. The laser heat source S (Wm^{-3}) was assumed to be Gaussian and is expressed as:

$$S(z,t)=I(t)(1-R_i)\alpha_i\exp(-\alpha_i z). \tag{3}$$

R is the reflectivity, α is the optical absorption coefficient, and $I(t)$ is the laser intensity.

Solution of Eq. (1) in each region (air, film, glass) has to be found taking into account the continuity of both temperature and normal component of heat absorbed by the sample at the boundaries.

A dimensionless absorption coefficient β in terms of thermal heat wave propagation w in thin film can be written as [12]:

$$\beta = 2wt_k\alpha, \tag{4}$$

where t_k is the time traversed in the film, depending on its thermal conductivity. The following variable was taken for skin depth z of sample as, in order to allow the use of dimensionless equation:

$$\chi=\frac{wz}{2\alpha}. \tag{5}$$

Laplace transformation of the characteristic Eq. (1) will be performed and analytical solution (Van Neumann condition) can be found taking into account the initial and boundary conditions of both thin film and thick substrate (glass). Analytical solution is in the form of [12]:

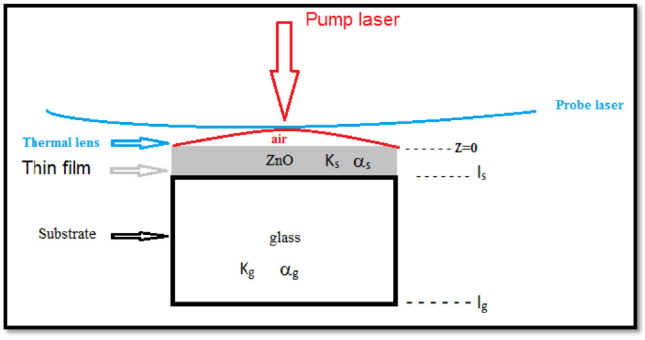

Fig. 1. Schematic drawing of the plane view of undoped-ZnO thin film grown on glass substrate. Pump-probe and thermal lens involved on the sample are shown.

$$\theta(\chi,u)=\frac{2\beta\psi_o\eta(u+2)\exp(-\beta l)}{\left(u(u+2)-\beta^2\right)[-u(u+2)]^{\frac{1}{2}}\cos(\lambda l)}\sin(\lambda l) + \frac{2\psi_o\eta(u+2)}{u(u+2)-\beta^2}\exp(-\beta l), \tag{6}$$

where θ is the dimensionless temperature, η is the dimensionless energy density absorbed in the medium, and u is the Laplace variable.

Solving the above equation numerically to estimate the temperature elevation and hence energy density absorbed in the both thin film and the substrate. The solution is shown in Fig. 2. Energy density absorbed by the sample of one layered undoped-ZnO as a function of depth with absorption of glass as a substrate, shows an exponential decrease upto the interface. The increase in the glass temperature started in the ZnO rather than at the interface. The figure shows also the discontinuity in the temperature elevation at the ZnO-glass interface.

3. Experiments

Undoped-ZnO thin films were deposited by CVD on glass substrate, since for high-quality ZnO has to be deposited on other substrates and has the advantage of thermodynamic dependent growth and control at the atomic level [16]. Structural characteristics, surface morphology, interfacial structure, and thermal stability, are evaluated. Generally, undoped ZnO thin films show n-type conductivity [17]. The samples were deposited at high temperature in order to remove the amorphous and crystalline phases [18].

Structure analysis of the thin films was performed with X-ray diffraction (XRD) using Cu radiation of wavelength ($\lambda(k_\alpha) = 0.1548$ nm). For optical transmittance, FTIR spectrometer in the range of 350–1100 nm was used. SEM of the samples was also carried out. These experiments were necessary to assess and confirm that thin films with high quality and grain size in the limit of nanoscale had been deposited. For thermal induced effects on the surface of thin film, optical absorption or refractive index change with temperature, and thermal properties such as thermal diffusivity of ZnO were studied thoroughly with the technique of photothermal deflection. The pump laser was a CW of power 5 mW, diode-pumped solid-state (DPSS) Nd:YAG at the second harmonic wavelength 532 nm. The laser was modulated at a frequency of 40.2 Hz by a mechanical chopper (Thorlab Model MC1000) and then focused on the sample surface. The probe beam was a He–Ne laser of 632.8 nm wavelength with a power output of 1 mW. A position sensor (bi-cell photodiode) was used to determine the amplitude and phase of the probe beam deflection. The output of the position sensor was fed into the lock-in amplifier (EG&G Princeton Applied Research Model 5209) via a differential detecting and amplifying circuit. A reference frequency from the mechanical chopper was connected to the lock-in amplifier. The sample holder for the ZnO was mounted on a three-axes inclination micro-positioning device. The signal was then recorded by the digital storage oscilloscope (UT 2102C). Repeated measurements were taken to minimize the noise. Lenses were used to focus the beams in an accurate manner after choosing the appropriate focal lengths, and they were also used to adjust the focal waists of the beams.

4. Results and discussion

4.1. Structure and optical study

Scanning electron microscope (SEM) is the convenient procedure to assess the surface morphology and microstructure of thin

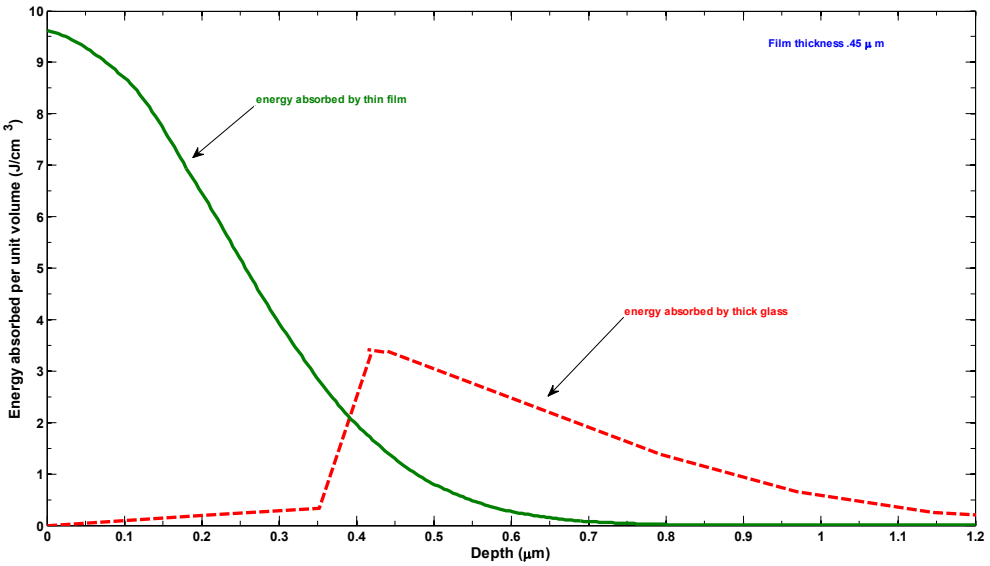

Fig. 2. Energy density absorbed by undoped-ZnO and the glass substrate versus the skin depth of the sample illuminated by pump laser of power 5 mW and wavelength 532 nm.

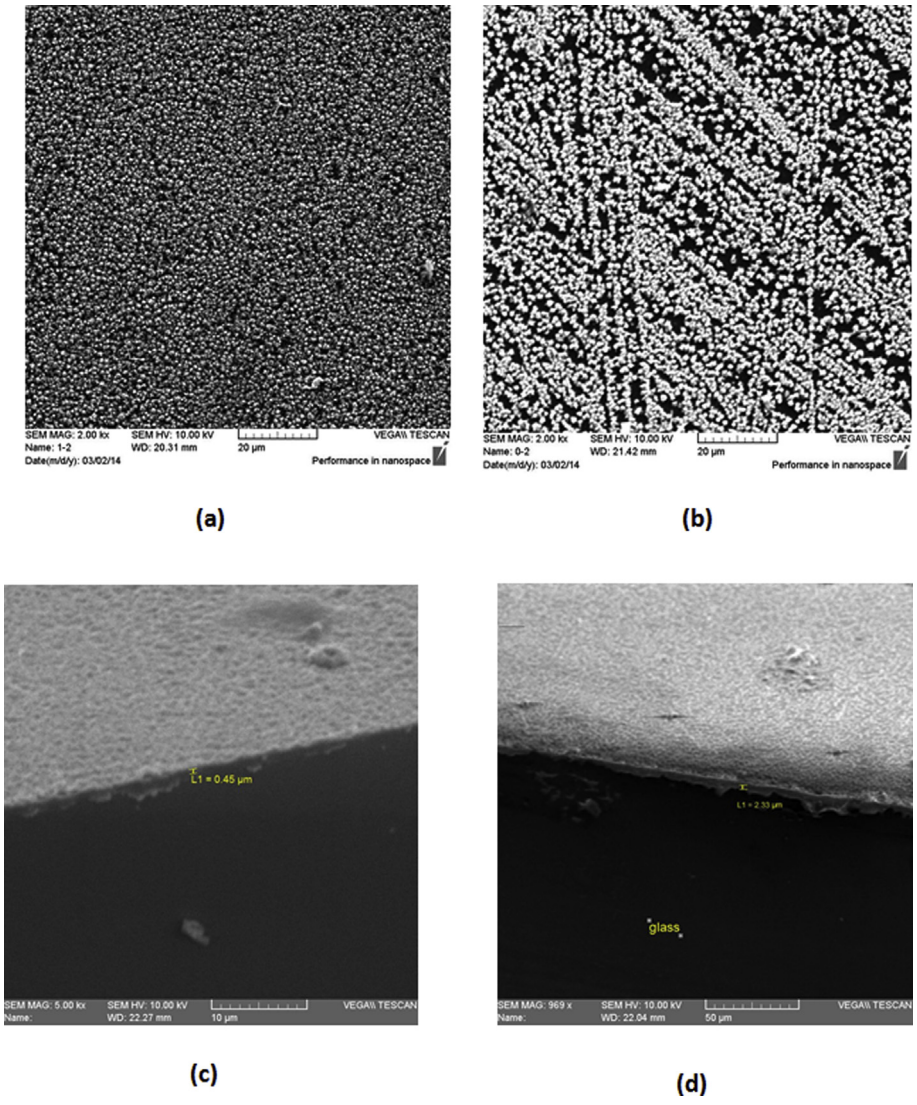

Fig. 3. SEM of undoped-ZnO .(a) Sample of group #1,(b) sample of group #2, (c) cross-sectional SEM image of (a), and (d) cross-sectional SEM image of (b).

films. The SEM micrographs of both group #1 & group #2 were examined. Group #1 samples showed a formation of micrometer crystallites distributed uniformly over the surface, as shown in Fig. 3a, while group #2 is shown in Fig. 3b, for one of the samples examined. It can be seen that, group #1, the grains were packed closely and distributed on the glass substrate. The SEM of group #2 shows a nonunifrom distribution and gathered in clusters. Cross-sectional image sample of group #1 is shown in Fig. 3c, where group #2 samples as in Fig. 3d.

Surface quality and homogeneity of the films were also confirmed by both PDT and transmission spectra for high quality samples of (group #1) except for few samples as will be shown in the article, i.e., (group #2). The X-ray diffraction spectra of the undoped-ZnO samples were revealed and the grain size D from the data was calculated using Debye-Scherrer formula [19,20]:

$$D = \frac{0.9\lambda(k_\alpha)}{\beta \cos\theta}, \tag{7}$$

where β the broadening of diffraction line is measured at the half maximum intensity in radians and θ is the angle of diffraction. The texture coefficient [19] of the plane (002) was calculated to be of the highest value for group #1 and with lowest value for group #2.

The transmittance optical spectra of the samples were recorded, as shown in Fig. 4 by FTIR spectrometer. In UV region, we can observe that the transmittance of group #1 had started from 350 nm while group #2 started from 380 nm. A sharp increase in the transmittance indicating a direct transition in group #1 with nonlinearity being observed in the high transparency in the visible region. Group #2 showed a poor transmittance in visible region with a pronounced peaks in the near IR and sharp cutoff near 1100 nm. A ZnO film with high transmittance in visible region comes from the fact it is a direct and wide band gap semiconductor.

Direct optical band gap energies of the samples can be derived from the difference between the edges of the valence band and conduction band (Tauc gap) as [21]:

$$(\alpha h\nu)^n = \mathbb{C}(h\nu - E_o), \tag{8}$$

where $h\nu$ is the photon energy, E_o the optical band gap energy of the semiconductor, and $\mathbb{C}$ is a constant. The value of the exponent n denotes the nature of the transition; $n = 2$ for direct transition and $n = 1/2$ for indirect transition.

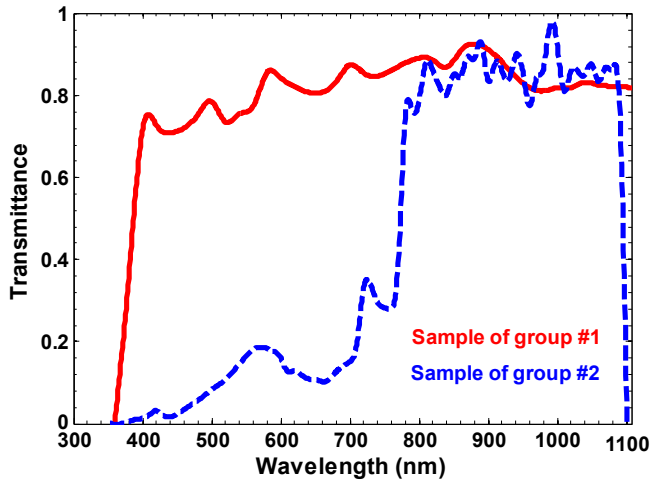

Fig. 4. Optical transmittance of undoped-ZnO thin films for both groups #1 & #2.

Fig. 5 represents the variation of $(\alpha.h\nu)^2$ with the photon energy of the undoped-ZnO thin films. The sample of group #1 shows an energy a band gap of 3.32 eV, which is in agreement with many reported results, e.g., Kang et al. [22]. The energy was calculated from the interception (extrapolation) of the straight line to zero absorption coefficients on the energy axis. This indicates the direct band gap transition. While the sample of group #2 shows a peculiar behavior rather than a straight line, and if an extrapolation could be done on the characteristic curve, an energy band gap of 3.023 eV would be obtained. The reduction in the energy gap, and it is difficulty to obtain, for the sample of group #2 suggested the poor crystal quality, and the disorder in the deposited film. This will lead to low transmittance in the visible region, Fig. 4, and strong phonon scattering due to the existence of gathered in clusters in the film.

The variation of refractive indices of both groups had been calculated from the transmittance and absorbance [23], and drawn as in Fig. 6. Refractive index is one of the fundamental properties for an optical material, because it is closely related to the electronic polarizability of ions and the local field inside materials [23]. The refractive index of group #1 shows a decrease with the increasing wavelength in the visible region and kept unvaried up to the near IR, while group #2 shows a step decrease of refractive index in the visible region and a sharp increase in the near IR. The sharp increase in the refractive index is due to high density of the films and could be calculated using Lorentz–Lorenz model [24].

4.2. Photothermal deflection technique

The dependence of the photothermal deflection on the modulated frequency of the pump laser is shown in Fig. 7. The deflection had decreased with increasing chopping frequency indicating that the temperature of the ZnO thin film in the central region had decreased. The decrease in the photothermal deflection was found to have a quadratic rather than linear dependence on the square of the frequency for both groups, especially for sample of group #2, because the thermal length also decreased, preventing the heat from reaching the probe beam [25]. The technique utilizes the refractive index gradient generated as a result of the absorption of intensity modulated pump laser. Still group #2 shows a different behavior from group #1 and with higher deflection due to more thermal length associated heat excitation Thermal waves) by the pump power.

Thermal change of the refractive index of the undoped-ZnO films will be revealed. The configuration depicted in Fig. 1 where sample/air interface is at $z = 0$. The thermal lens was acquired as a relative change in the laser probe beam intensity as [25]:

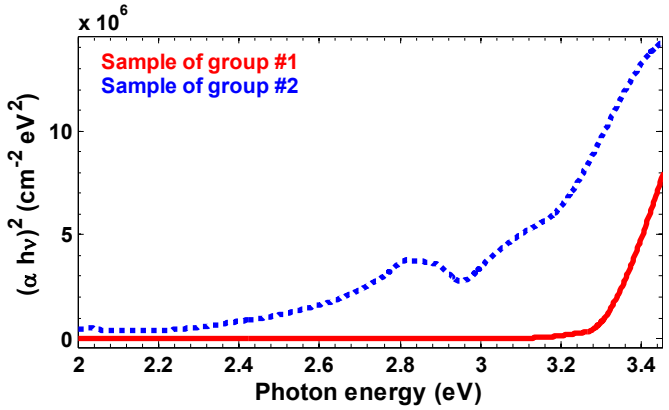

Fig. 5. Variation of $(\alpha.h\nu)^2$ with photon energy of the undoped-ZnO thin films.

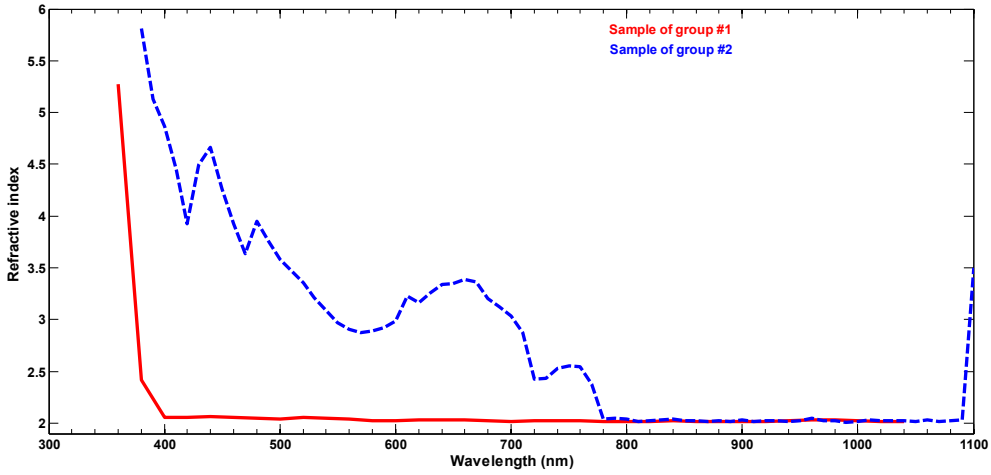

Fig. 6. Refractive index change with wavelength of undoped-ZnO films.

$$\vartheta(t) = 4\left(\frac{P_p}{w_e^2}\right) \times B(t) \times E_o D_s \times \alpha_s l_s, \tag{9}$$

where P_p is the laser pump power, w_e is the beam waist radius of pump laser, $B(t)$ is the time-dependent geometrical constant [26], l_s is the sample (thin film) thickness, and E_o is given by [25];

$$E_o = \frac{-\frac{dn_s}{dT}}{\lambda_p k_s}. \tag{10}$$

The heat flow is one dimensional as regarded in Eq. (1), and at times long after the end of pump laser pulse heating, the temperature of the thin film is considered uniform. The temperature will decay exponentially and the heat will flow to the substrate, as shown in Fig. 2. The time constant t_c is defined as [27]:

$$t_c = \frac{w_e}{4D_s}. \tag{11}$$

The time-dependent photothermal deflection in Eq. (9) can be written now as:

$$\vartheta(t) = P_p \times \frac{B(t)}{t_c} \times E_o \times \alpha_s l_s. \tag{12}$$

Hence, the deflection decays with time, and the change in refractive indices of the films with temperature shown in Eq. (10) will be evaluated besides the thermal diffusivity of the thin films.

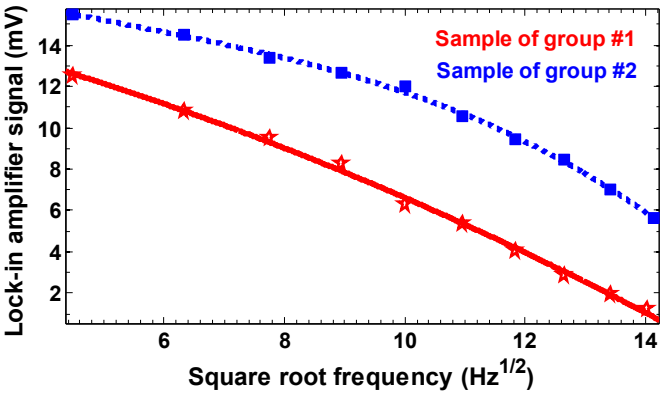

Fig. 7. Photothermal deflection of undoped-ZnO films as a function of square root of pump laser frequency.

Thermal change in refractive index of undoped-ZnO thin film is an important parameter regarding its effect on the application for solar cells and flat panel displays. Refractive indices of both groups #1 & 2 as a function of temperature are shown in Fig. 8.

The refractive index change of undoped-ZnO of group #1 with temperature was estimated with curve fitting, assuming linear decrease, as $(-4.5 \times 10^{-3}/\mathrm{K})$. For samples of group #2, the variation of refractive index with increasing temperature was estimated as $(-19 \times 10^{-3}/\mathrm{K})$. The temperature increase was monitored as a result of the power increment of laser pump power. The deformation in the surface of the sample at high temperature is obvious in group #2. Photothermal deflection technique can provide, in addition to the possibility of measuring the temperature variation of refractive index, it allows the determination of a relationship between the heating of the material (by pump power) and its deformation response to the laser pump.

The contribution of thermal perturbation is the dominant effect on the deflection of probe laser arises at low chopping frequency (40.2 Hz) of the pump laser, as follows [28]:

$$\text{deflection} \propto \frac{1}{n_s}\frac{dn_s}{dT}\frac{dT(z,t)}{dz}. \tag{13}$$

The change of refractive index of group #2 shows a high index gradient with temperature due to its high thermal diffusivity change temperature. Thermal lens effect is caused by deposition of heat via a non-radiative decay process after laser energy has been absorbed by the sample, resulting in a spreading of the beam and a reduction in the intensity at the beam center (dn_s/dT is negative) [29].

Thermal diffusivity (D_s) of undoped-ZnO films were evaluated by experimental investigation from the slope of the linear relation between the phase of a periodically deflecting beam as a function of the separation between laser pump and laser probe [30]. The estimated value for group #1 was 4.354×10^{-2} cm^2/s while for group #2 was 5.035×10^{-2} cm^2/s. The difference in the values of (D_s) of the two groups is related to the difference in the thickness of the films. Thermal resistivity of the thin film substrate interface had an influence on the measured thermal diffusivity by the PDT [31].

5. Conclusions

Optical and thermal measurements of undoped-ZnO thin films have been carried out. It is seen that films of thickness of submicron (0.45 μm and less) show the required behavior for such films

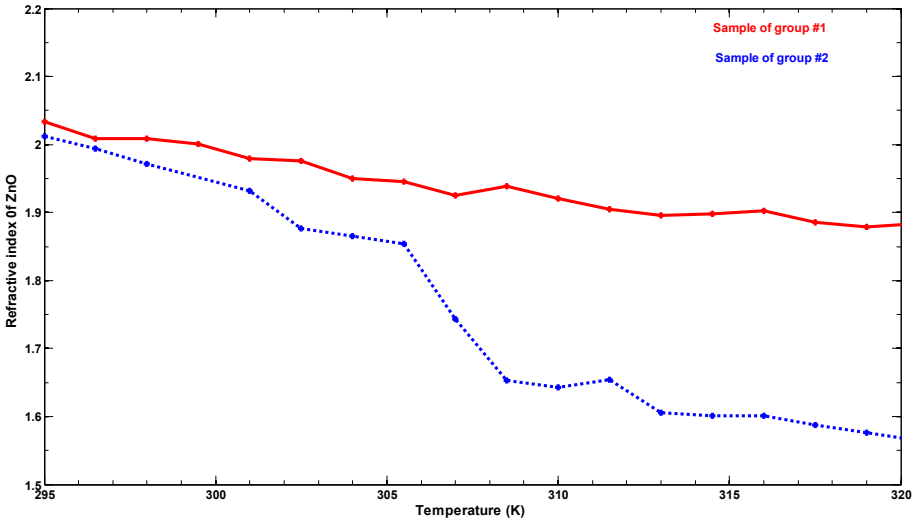

Fig. 8. The variation of refractive index of undoped-ZnO thin films with temperature.

regarding their applications. Films of thickness (1–2.33 μm) show a substantial reduction in the band gap energy, a pronounced peak of the transmittance in the near IR and sharp cutoff of the transmittance near 1100 nm, and a step decrease of refractive index in the visible region and a sharp increase in the near IR. The films of group #2, of a nonuniform distribution and gathered clusters, resulting in a layered structure will be affected by the phonons and their scattering mechanism. This mechanism had been investigated further by photothermal deflection technique and its influence on the thermal properties of the thin films. Temperature gradient of refractive indices of both group #1 and group #2 were (-4.5×10^{-3}/K) and (-19×10^{-3}/K), respectively. Thermal diffusivity for group #1 was found as 4.354×10^{-2} cm^2/s while for group #2 was 5.035×10^{-2} cm^2/s. This can be interpreted as an additional scattering of phonons in the layered structure and thermal resistivity of the thin film substrate interface. The refractive index variation with temperature and thermal diffusivity do not agree with any data in the literature (to our knowledge). A discontinuity in the temperature elevation at the ZnO-glass interface was found by numerical simulation of one-dimensional heat equation.

Acknowledgment

We are grateful to M.I. Manssor for device fabrication by CVD of the comparative set of ZnO samples.

References

[1] H.-T. Huang, C.-Yu Huang, T.-R. Ger, Z.–H. Wei, Anti-integrin and integrin detection using the heat dissipation of surface plasmon resonance, Appl. Phys. Lett. 102 (2013) 111109.
[2] M.R. Ferdinandus, H. Hu, M. Reichert, D.J. Hagan, E.W. Van Stryland, Beam deflection measurement of time and polarization resolved ultrafast nonlinear refraction, Opt. Lett. 38 (18) (2013) 3518.
[3] L.M. Cervantes-Espinosa, F. de L. Castillo-Alvarado, G. Lara Hernández, A. Cruz-Orea, C. Hernández-Aguilar, A. Domínguez-Pacheco, Thermal effusivity of vegetable oils obtained by a photothermal technique, Int. J. Thermophys. 33 (12) (2012) 2243.
[4] A. Gutierrez-Arroyo, C. Sanchez-Perez, N. Aleman-Garcia, Optical sensor for heat conduction measurement in biological tissue, J. Phys. Conf. Ser. 450 (2013) 012027.
[5] K.I. Mohammad, M.I. Azawe, The development of a novel technique to evaluate the CR-39 track response to alpha particles, Turk. J. Phys. 37 (2013) 182.
[6] I. Gaied, A. Gassoumi, M. Kanzari, N. Yacoubi, Investigation of thermal properties of sulfosalt $SnSb_2S_4$ thin films by the photothermal deflection technique, J. Phys. D. Conf. Ser. 214 (2010) 012052.
[7] W. Lee, S. Shin, D.-R. Jung, J. Kim, C. Nahm, T. Moon, B. Park, Investigation of electronic and optical properties in Al-Ga codoped ZnO thin films, Curr. Appl. Phys. 12 (2012) 628.
[8] U. Alver, W. Zhou, A.B. Belay, R. Krueger, K.O. Davis, N.S. Hickman, Optical and structural properties of ZnO nanorods grown on graphene oxide and reduced graphene oxide film by hydrothermal method, Appl. Surf. Sci. 258 (2012) 3109.
[9] D.C. Look, Recent advances in ZnO materials and devices, Mater. Sci. Eng. B 80 (2001) 383.
[10] C. Li, M. Furuta, T. Matsuda, T. Hiramatsu, H. Furuta, T. Hirao, Effects of substrate on the structural, electrical and optical properties of Al-doped ZnO films prepared by radio frequency magnetron sputtering, Thin Solid Films 517 (11) (2009) 3265.
[11] A. Shukla, V.K. Kaushik, D. Prasher, Growth and characterization of $Mg_xZn_{1-x}O$ thin films by aerosol-assisted chemical vapor deposition (AACVD), Electron. Mater. Lett. 10 (1) (2014) 61.
[12] F.M. Jasim, M.I. Azawe, Parametric variations of analytical solution of dual phase lag heat conduction equation, Acad. J. Sci. Res. 1 (2) (2013) 29.
[13] I. Gaeid, A. Guassoumi, M. Kanzari, N. Yacoubi, Investigation of optical properties of $SnSb_2S_4$ and $Sn_2Sb_2S_5$ thin films by a non destructive technique based on the photothermal deflection spectroscopy, in: 10th Int. Conf. Slovenian Soc.. For Non-destructive Testing, Sept. 1-3 2009, p. 493 (Ljubljana, Slovenia).
[14] L. Wu, A. Knoesen, Absolute absorption measurement of polymer for optical waveguide applications by photothermal deflection spectroscopy, J. Polym. Sci. 39 (2001) 2717.
[15] J. Hong, S.H. Kim, D. Kim, Effect of laser irradiation on thermal conductivity of ZnO nanofluids, J. Phys. Conf. Ser. 59 (2007) 301.
[16] C.R. Gorla, N.W. Emanetoglu, S. Liang, W.E. Mayo, Y. Lu, M. Wraback, H. Shen, Structural, optical, and surface acoustic wave properties of epitaxial ZnO films grown on $(01\bar{1}2)$ sapphire by metalorganic chemical vapor deposition, J. Appl. Phys. 85 (5) (1999) 2595.
[17] D. Kim, I. Yun, H. Kim, Fabrication of rough Al doped ZnO films deposited by low pressure chemical vapor deposition for high efficiency thin film solar cells, Curr. App. Phys. 10 (2010) S459.
[18] S.T. Tan, B.J. Chen, X.W. Sun, W.J. Fan, H.S. Kwok, X.H. Zhang, S.J. Chua, Blueshift of optical band gap in ZnO thin films grown by metal-organic chemical-vapor deposition, J. Appl. Phys. 98 (2005) 013505.
[19] S. Ilican, M. Caglar, Y. Caglar, Determination of the thickness and optical constants of transparent indium-doped ZnO thin films by envelope method, Mat. Pol. 25 (3) (2007).
[20] B.D. Cullity, S.R. Stock, Elements of X-ray Diffraction, third ed., Prentice Hall, New York, 2001.
[21] O. Stenzel, The Physics of Thin Film Optical Spectra: An Introduction, Springer-Verlag, Berlin Heidelberg, Germany, 2005.
[22] H.S. Kang, J.S. Kang, J.W. Kim, S.Y. Lee, Annealing effect on the property of ultraviolet and green emissions of ZnO thin films, J. Appl. Phys. 95 (2004) 1246.
[23] S.W. Xue, X.T. Zu, W.L. Zhou, H.X. Deng, X. Xiang, L. Zhang, H. Deng, Effects of post-thermal annealing on the optical constants of ZnO thin film, J. Alloys Compd. 448 (2008) 21.
[24] E. Elangovan, K. Ramamurthi, Optoelectronic properties of spray deposited SnO_2:F thin films for window materials in solar cells, J. Optoelect. Adv. Mat. 5 (2003) 45.
[25] D.A. Nedosekin, N.V. Saranchina, A.V. Sukhanov, N.A. Gavrilenko, I.V. Mikheev, M.A. Proskurnin, Solid phase-enhanced photothermal lensing with

mesoporous polymethacrylate matrices for optical-sensing chemical analysis, Appl. Spectrosc. 67 (2013) 1.
[26] R.D. Snook, R.D. Lowe, Thermal lens spectrometry – a review, Analyst 120 (1995) 2051.
[27] K.I. Mohammed, M.I. Azawe, Measurement of thermal and optical properties of CR-39 solid-state nuclear detector by photothermal deflection, Nucl. Instrum. Methods Phys. Res. B 308 (2013) 54.
[28] S.E. Bialkowski, Photothermal Spectroscopy Methods for Chemical Analysis, Wiley, New York, 1996, ISBN 0-471-57467-8.
[29] E. Shahriari, W.M. Mat Yunus, R. Zamiri, The effect of nanoparticle size on thermal diffusivity of gold nano-fluid measured using thermal lens technique, JJ. Eur. Opt. Soc. Rap. Public 8 (2013) 13026.
[30] A.E. Aliev, Y.N. Gartstein, R.H. Baughman, Mirage effect from thermally modulated transparent carbon nanotube sheets, Nanotechnology 22 (2011) 435704.
[31] S. Ktifa, A. Souissi, F. Saadallah, V. Sallet, M. Oueslati, N. Yacoubi, photothermal investigation study of ZnO thin films: effects of Zn and O polar substrate, Appl. Phys. A 114 (2014) 559.